Evolutionary trends of physical properties of protostellar cores in high-mass star-forming regions revealed by ALMA

Caroline Gieser
(gieser@mpe.mpg.de)

Caroline Gieser[1,2] ,
Henrik Beuther[2], Dmitry Semenov[2], Aida Ahmadi[3], Thomas Henning[2], and Molly Wells[2]

[1]Max-Planck-Institut für extraterrestrische Physik, Giessenbachstrasse 1, 85748 Garching, Germany
[2]Max Planck Institute for Astronomy, Königstuhl 17, 69117 Heidelberg, Germany
[3]Leiden Observatory, Leiden University, P.O. Box 9513, 2300 RA Leiden, the Netherlands

based on: Gieser+2023a (A&A 674, A160)

SUMMARY

High-mass star formation is a hierarchical process from cloud (>1 pc), to clump (0.1-1 pc) to core scales (<0.1 pc). Modern interferometers achieving high angular resolutions at mm wavelengths allow us to probe the physical and chemical properties of the gas and dust of protostellar cores in the earliest evolutionary formation phases from infrared dark clouds (IRDCs), high-mass protostellar objects (HMPOs), hot molecular cores (HMCs), to ultra-compact (UC)HII regions.

In this study, we investigate how physical properties, such as the density and temperature profiles, evolve on core scales through the evolutionary sequence during high-mass star formation ranging from protostars in cold IRDCs to evolved UCHII regions. We observed 11 high-mass star-forming regions with ALMA (PI: Caroline Gieser) at 3 mm wavelengths (**→ Figure 2**). Based on the 3 mm continuum morphology and H(40)α recombination line emission, tracing locations with free-free (ff) emission, the fragmented cores analyzed in this study are classified into either "dust cores" or "dust+ff cores". In addition, we resolve three cometary UCHII regions with extended 3 mm emission that is dominated by free-free emission. The temperature distribution and radial profiles (**$T \sim r^{-q}$**) are determined by modeling molecular emission of CH_3CN and $CH_3^{13}CN$ with XCLASS and by using the HCN-to-HNC intensity ratio as probes for the gas kinetic temperature. The density profiles (**$n \sim r^{-p}$**) are estimated from the 3 mm continuum visibility profiles.

Including the results of the CORE and CORE-extension studies with NOEMA (Gieser+2021,2022) to increase the sample size, we find evolutionary trends on core scales for the temperature power-law index q increasing from 0.1 to 0.7 from infrared dark clouds to UCHII regions, while for the density power-law index p on core scales, we do not find strong evidence for an evolutionary trend. However, we find that on the larger clump scales throughout these evolutionary phases the density profile flattens from p ≈ 2.2 to p ≈ 1.2 consistent with findings from Beuther+2002,2023.

By characterizing a large statistical sample of individual fragmented cores, we find that the physical properties, such as the temperature on core scales and density profile on clump scales, evolve even during the earliest evolutionary phases in high-mass star-forming regions. Our findings provide observational constraints for theoretical models of the formation of massive stars. In follow-up studies we aim to further characterize the chemical properties of the regions by analyzing the large amount of molecular lines detected with ALMA (**→ Figure 1**) in order to investigate what processes drive the chemical evolution in high-mass star-forming regions.

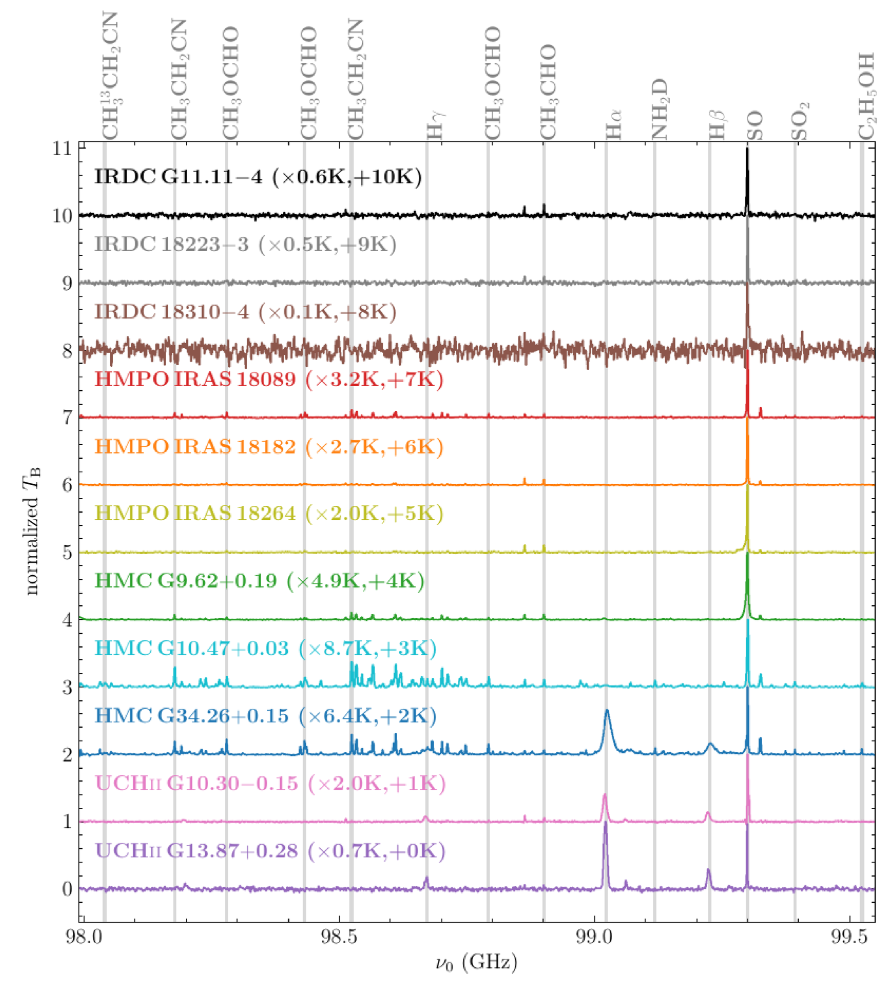

Figure 1. Mean spectra of the regions in one spectral window (normalized to SO peak intensity). The entire spectral range of this ALMA project covers ~10 GHz at 3 mm within 39 spectral windows.

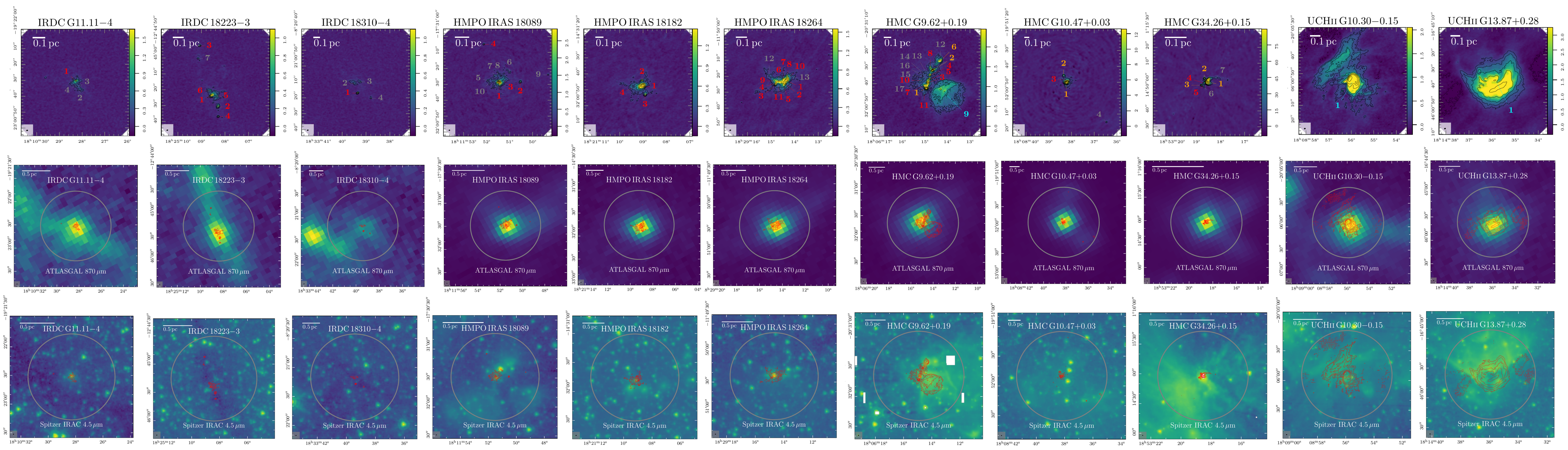

Figure 2. Multi-wavelength overview of the sample in comparison with the new high angular resolution ALMA 3mm data.
Top row: The ALMA 3mm continuum data is shown in color and in black contours. Fragmented objects are classified and labeled as compact cores that are dominated by dust emission (''dust cores'') in red, compact cores with dust+ff emission (''dust+ff cores'') in orange, and cometary UCHII regions with extended ff emission in cyan. Cores with S/N < 15 are not analyzed in this work and are labeled in grey.
Central and bottom row: The ATLASGAL 870µm and Spitzer 4.5µm is shown in color, respectively. The ALMA 3mm continuum is shown in red contours and the grey circle highlights the ALMA 3mm primary beam size.

Temperature profiles

- temperature maps created using the HCN-to-HNC intensity ratio tracing material from 15 K – 50 K (Hacar+2020)
- CH_3CN and $CH_3^{13}CN$ temperature maps created with XCLASS (Möller+2017) tracing temperatures up to 250 K
- radial temperature profiles of the cores are fitted assuming a power-law profile:

$$T(r) = T_{\rm in} \times \left(\frac{r}{r_{\rm in}}\right)^{-q}$$

- an example for core 1 in IRAS 18089 is shown in **Figure 3**

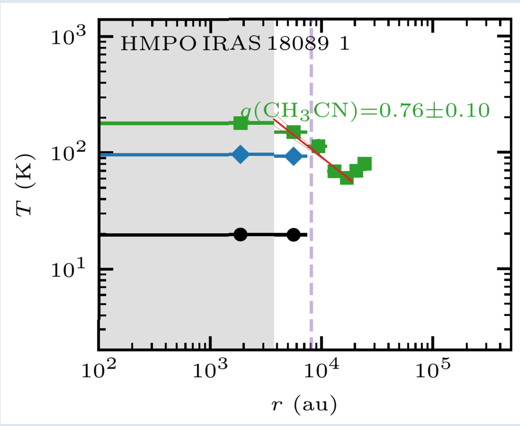

Figure 3. Radial temperature profile derived with CH_3CN (green), $CH_3^{13}CN$ (blue), and the HCN-to-HNC intensity ratio (black).

Density profiles

- assuming that the density profile follows a power-law profile:

$$n(r) = n_{\rm in} \times \left(\frac{r}{r_{\rm in}}\right)^{-p}$$

and that the 3mm continuum visibility profile as a function of uv distance s (**$V \sim s^{\alpha}$**) stems from optically thin dust emission, the power-law indices are related by:

$$\alpha = p + q - 3$$

- **Figure 4** shows as an example the visibility profile for the dust+ff core 2 in HMC G34.26+0.15. For most of the cores, two power-law profiles, on the clump and core scales, respectively, were observed and fitted.

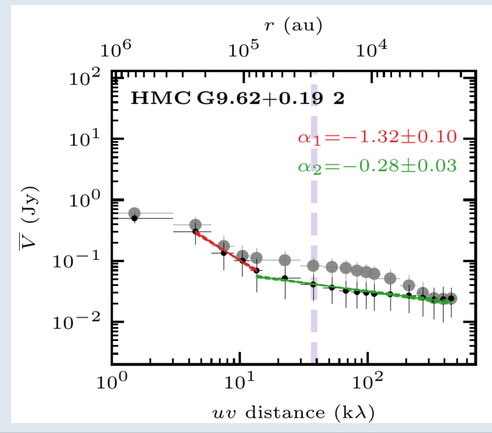

Figure 4. Visibility profile of the 3mm continuum with a fit on clump (α_1, red) and core scales (α_2, green).

Evolutionary trends of physical parameters on clump and core scales

Do we find evolutionary trends on clump scales (→ Figure 5)?
The dust temperature (taken from Urquhart+2018) increases from 10 K to 35 K from IRDCs to UCHII regions. The 3mm peak intensity increases only from IRDCs to HMCs and then decreases by 1-2 orders of magnitudes for UCHII regions. This can be explained by the expanding UCHII regions resulting in a lower surface brightness (**Figure 2**).

Do we find evolutionary trends on core scales (→ Figure 6)?
The temperature at 1000 K is increasing from cores in the IRDCs to HMC stage and at the same time, the profile becomes steeper with q increasing from 0.1 to 0.7. We do not find clear evidence for evolutionary trends of the density profile on core scales, p_2.

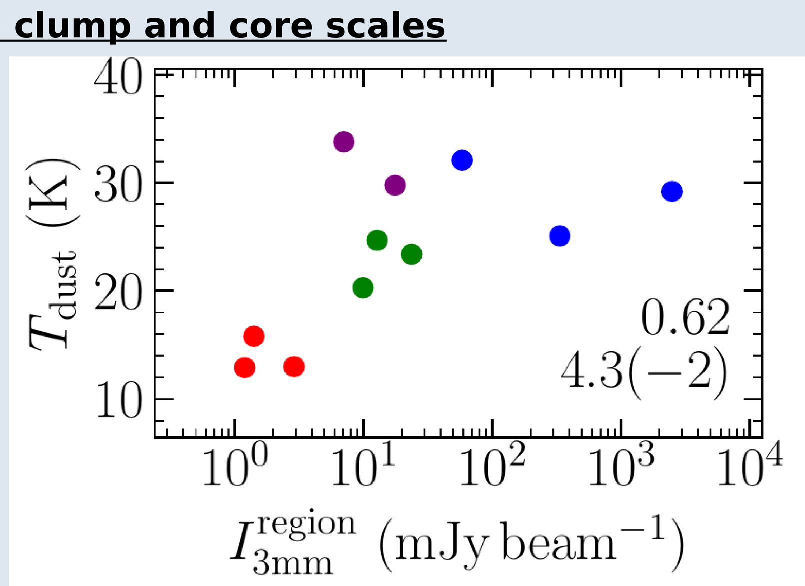

Figure 5. Parameters on clump scales. Comparison of the ALMA 3mm peak intensity (this work) with the dust temperature (Urquhart+2018). In color, the evolutionary stage is highlighted (red: IRDC, green: HMPO, blue: HMC, purple: UCHII).

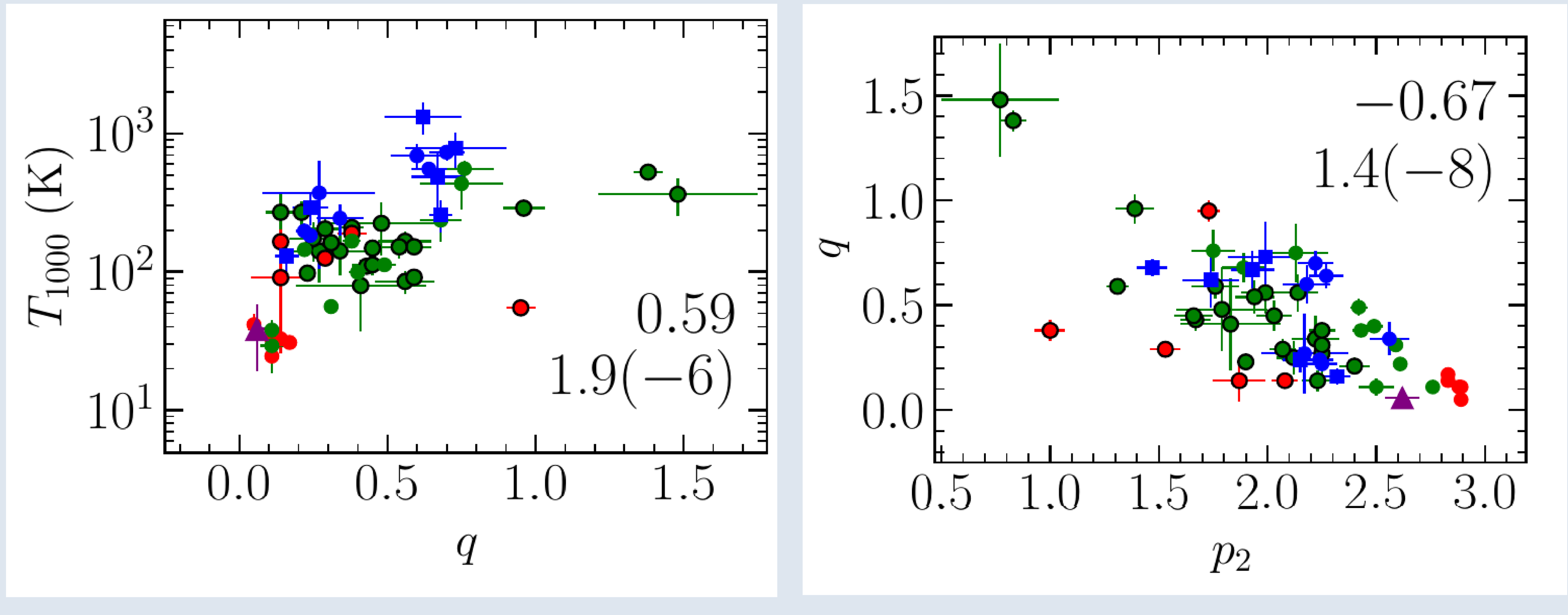

Figure 6. Parameters on core scales: temperature at 1000au, T_{1000}, temperature and density power-law index on core scales, q and p_2. In color, the evolutionary stage is highlighted (red: IRDC, green: HMPO, blue: HMC, purple: UCHII). Dust cores are marked by circles, dust+ff cores by squares, and the cometary UCHII region by a triangle. Dust cores studied within the CORE and CORE-extension projects with NOEMA 1mm observations (Gieser+2021, 2022) are enclosed in black circles.

→ The clump properties (Figure 5) show distinct regions for each evolutionary stage. On core scales, there is a significant overlap of cores in different phases (Figure 6). This is because multiple cores at different evolutionary stages can be present within a single clustered region (e.g., G09.62+0.19, Figure 2). We as a community should work on an improved classification scheme taking into account that we can now study the core scales in large samples in high-mass star-forming regions.

Outlook

In this first project, we analyzed the physical properties of fragmented sources in 11 high-mass star-forming regions using mainly the 3mm continuum data and a few selected emission lines (Hα, HCN, HNC, CH_3CN, $CH_3^{13}CN$). However, this project covers in total ~10 GHz of spectral bandwidth and there is a huge diversity in molecular lines (**→ Figure 1** shows a small part of a spatially averaged spectrum toward each region).
In follow up studies we will therefore investigate the chemical properties, how molecular abundances evolve and how they connect to the underlying physical properties.

References:

Beuther, H., Schilke, P., Menten, K. M., et al. 2002, ApJ, 566, 945
Beuther, H., Gieser, C., Soler, J. D., et al. 2023, A&A, in press
Gieser, C., Beuther, H., Semenov, D., et al. 2021, A&A, 648, A66
Gieser, C., Beuther, H., Semenov, D., et al. 2022, A&A, 657, A3
Gieser, C., Beuther, H., Semenov, D., et al. 2023, A&A, 674, A160
Hacar, A., Bosman, A. D., & van Dishoeck, E. F. 2020, A&A, 635, A4
Möller, T., Endres, C., & Schilke, P. 2017, A&A, 598, A7
Urquhart, J. S., König, C., Giannetti, A., et al. 2018, MNRAS, 473, 1059